The application of inverse-dispersion and gradient methods to estimate ammonia emissions from a penguin colony

Mark R. Theobald , Peter D. Crittenden , Y. Sim Tang , Mark A. Sutton

HIGHLIGHTS

- We measure atmospheric ammonia concentrations at locations around a penguin colony.
- We estimate ammonia emission rates using inverse modelling and gradient methods.
- Mean ammonia emissions are estimated to be 1.1 g ammonia per breeding pair per day.
- We estimate that 2% of the nitrogen excreted by the penguins is emitted as ammonia.

GRAPHICAL ABSTRACT

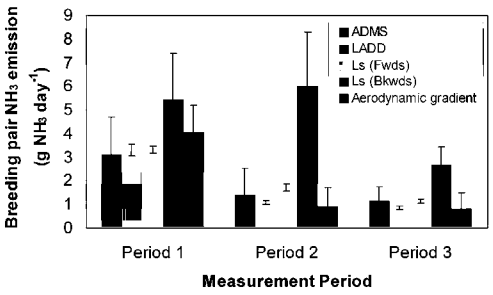

Keywords:
Ammonia emissions
Penguins
Seabirds
Inverse-dispersion modelling
Nitrogen

ABSTRACT

Penguin colonies represent some of the most concentrated sources of ammonia emissions to the atmosphere in the world. The ammonia emitted into the atmosphere can have a large influence on the nitrogen cycling of ecosystems near the colonies. However, despite the ecological importance of the emissions, no measurements of ammonia emissions from penguin colonies have been made. The objective of this work was to determine the ammonia emission rate of a penguin colony using inverse-dispersion modelling and gradient methods. We measured meteorological variables and mean atmospheric concentrations of ammonia at seven locations near a colony of Adélie penguins in Antarctica to provide input data for inverse-dispersion modelling. Three different atmospheric dispersion models (ADMS, LADD and a Lagrangian stochastic model) were used to provide a robust emission estimate. The Lagrangian stochastic model was applied both in 'forwards' and 'backwards' mode to compare the difference between the two approaches. In addition, the aerodynamic gradient method was applied using vertical profiles of mean ammonia concentrations measured near the centre of the colony. The emission estimates derived from the simulations of the three dispersion models and the aerodynamic gradient method agreed quite well, giving a mean emission of 1.1 g ammonia per breeding pair per day (95% confidence interval: 0.4–2.5 g ammonia per breeding pair per day). This emission rate represents a volatilisation of 1.9% of the estimated nitrogen excretion of the penguins, which agrees well with that estimated from a temperature-dependent bioenergetics model. We found that, in this study, the Lagrangian stochastic model seemed to give more reliable emission estimates in 'forwards' mode than in 'backwards' mode due to the assumptions made.

1. Introduction

Large colonies of wild animals can emit substantial quantities of ammonia (NH_3) into the atmosphere. This is especially true for colonies of seabirds such as penguins, which represent some of the most concentrated natural sources of atmospheric ammonia in the world (Wilson et al., 2004; Riddick et al., 2012). Most penguin colonies are situated in remote locations and hence the emitted ammonia can represent the principal source of atmospheric nitrogen (N) input into nearby ecosystems, making them interesting case studies of ecosystem N-cycling (Lindeboom, 1984; Crittenden et al., unpublished results). Although penguins and other seabirds contribute less than 2% of global NH_3 emissions (Riddick et al., 2012), the concentrated nature of seabird colony emissions can have important local ecological effects, the understanding of which is aided by knowing how much NH_3 is emitted. At the same time, seabird colonies provide a model system for studying NH_3 emission processes that largely excludes human management of the excreta, allowing the effects of climatic differences to be examined (Sutton et al., 2013).

Initial estimates of penguin ammonia emissions on a global scale were made by Blackall et al. (2007), who estimated total NH_3 emissions from all seabird species of 242 Gg NH_3 $year^{-1}$ using a simple bioenergetics model. Penguin species contributed most, accounting for around half of this total. This approach was subsequently modified by Riddick et al. (2012) to include an estimated temperature dependency and updated database of seabird colonies to produce a spatial emission inventory for seabird NH_3 emissions. Laboratory studies have also been carried out to estimate the potential of penguin colonies to emit NH_3 into the atmosphere. For example, Zhu et al. (2011) studied the NH_3 emission potential of guano and ornithogenic soils from penguin colonies and their dependence on temperature, pH and total nitrogen content. However, despite these advances in emission inventories and laboratory studies, no field-based estimates of NH_3 emissions from penguin colonies have been published.

The objective of this paper is to derive the first field-based emission estimates (and their uncertainty) of a penguin colony using different dispersion models and micro-meteorological methods.

2. Materials and methods

2.1. Colony location

Cape Hallett is situated at the southern end of Moubray Bay, northern Victoria Land, in the western Ross Sea (Fig. 1a) at the northern tip of the Hallett Peninsula (72° 19′ S, 170° 16′ E; Fig. 1b). At the northern tip of the Cape is the small spit of Seabee Hook (Fig. 1c), where a colony of Adélie penguins (*Pygoscelis adeliae*) is located.

The most recent estimate of the colony size is 39 000 breeding pairs, recorded in the breeding season 1998–1999 (Landcare Research, 2000). In addition to the breeding pairs, the colony also contains non-breeding adults and chicks. The colony occupies an area of approximately 33.2 ha covering most of the spit and part of the slopes of the Cape (Fig. 1c). During summer, the sea surrounding the spit partly melts, while to the east rise the steep slopes of the Hallett peninsula (Fig. 1b).

2.2. Measurements

During the experimental period (December 2005–January 2006), which was coincident with the penguin breeding season, mean atmospheric ammonia concentrations were measured at seven locations (Fig. 1c) using ALPHA passive diffusion samplers (Tang et al. 2001) mounted at a height of 1.5 m above ground. The height of 1.5 m was used so that the measurements were made close to the emitting surface but out of reach of the penguins. Samplers were exposed in triplicate at each site for three periods: 26th December 2005 to 10th January 2006, 11th to 17th and 17th to 23rd January 2006. Measurements at additional heights of 0.25,

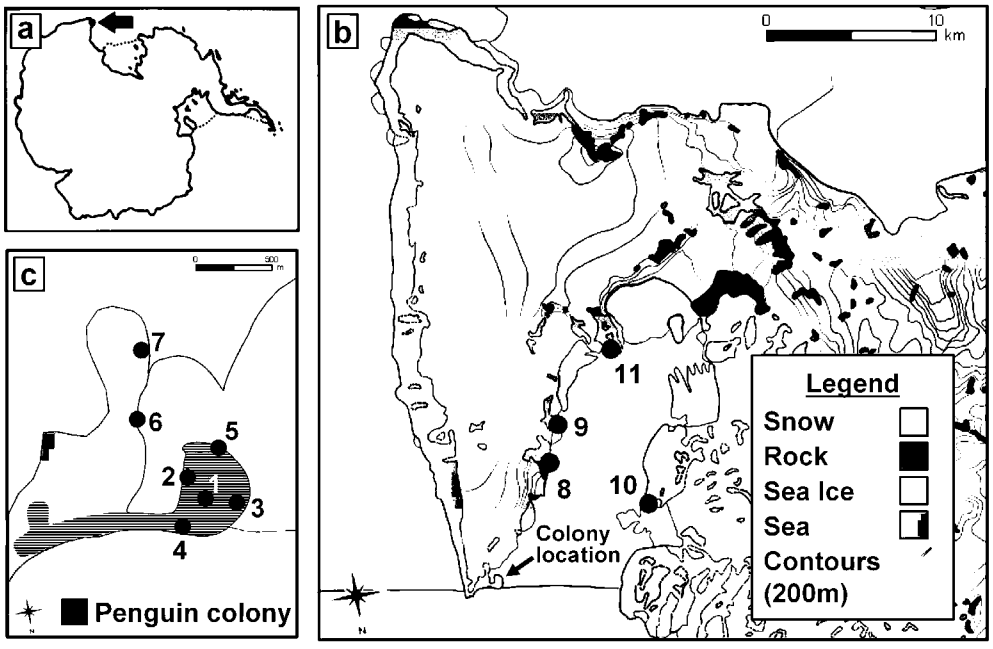

Fig. 1. Maps showing the locations of: a) the study site relative to the Antarctic continent; b) the Cape Hallett peninsula and c) the penguin colony. The numbered circles indicate the locations and site numbers of the ammonia concentration measurements. Note the rotated north directions in maps b and c. Land cover and contour data courtesy of the Antarctic Digital Database (ADD Consortium, 2000). Extent of sea ice and shape of Seabee Hook modified based on personal observations and aerial photographs, respectively.

0.63, and 2.5 m above ground level were also made at a site near the centre of Seabee Hook (site 1) for the calculation of emission rates using the aerodynamic gradient method. Samplers were also exposed at four remote locations during the first sample period to estimate background concentrations (sites 8–11, Fig. 1b).

Meteorological data were recorded at the long-term automatic meteorological station situated approximately 500 m east of the centre of the colony. The meteorological variables (air temperature, relative humidity, incoming and reflected solar radiation, wind speed and direction, minimum and maximum wind speed and the standard deviation of the wind direction) were logged every 15 min. Due to a damaged sensor, wind speed and direction data were not available for the first part of the first measurement period (up to 2nd January 2006).

2.3. Emission estimation methods

Many experimental techniques have been used to estimate emissions from a diverse range of (mostly agricultural) sources of NH_3 (see e.g. McGinn and Janzen (1998) for a review of commonly used methods). These techniques range from simple mean concentration vertical profile measurements (e.g. Misselbrook et al., 2005) to state-of-the-art eddy covariance systems requiring fast concentration sensors and accurate turbulence measurements (e.g. Famulari et al., 2004).

For application to penguin colonies, many of which are located in remote areas, a non-labour-intensive and non-resource-intensive (e.g. without mains power) technique is required. One such technique is the aerodynamic gradient method, which was used by Sutton et al. (2000) to estimate fluxes of NH_3 between an oilseed rape crop and the atmosphere. This method is based on the theoretical vertical concentration profiles of wind speed:

$$u(z-d) = \frac{u_*}{\kappa}\left[\ln\left(\frac{z-d}{z_0}\right) - \Psi_m\left(\frac{z-d}{L}\right)\right] \quad (1)$$

and concentration:

$$C(z-d) = \frac{C_*}{\kappa}\left[\ln(z-d) - \Psi_h\left(\frac{z-d}{L}\right)\right] - \text{const.} \quad (2)$$

where d is the displacement height, u_* is the friction velocity, κ is the Von Kármán constant (0.41), z_0 is the aerodynamic roughness length, L is the Monin–Obukhov length, C_* is a friction concentration and ψ_m and ψ_h are the stability corrections for momentum and heat, respectively. The emission flux is calculated from:

$$F = -u_* C_* \quad (3)$$

This method can be applied to both short (<1 h) and long (several days) averaging periods (conditional on limited variation in atmospheric stability, Famulari et al., 2010), making it suitable for experiments in remote locations.

For the long sampling periods used in this study, it was assumed that neutral conditions dominated and so the stability corrections of the aerodynamic gradient method (in Equations (1) and (2)) could be ignored (Sutton et al., 2000). The displacement height (d) was assumed to be zero in the absence of any vegetation canopy at the site.

Another non-resource-intensive estimation method makes use of inverse atmospheric dispersion modelling to relate mean atmospheric concentrations measured near the source to NH_3 emission rates. This technique is based on the assumption that atmospheric concentrations resulting from an emission source are directly proportional to the emission rate, thus for a perfect dispersion model it can be inferred that the real emission rate

$$Q = \frac{(C_{meas} - C_{bg})}{(C_{sim}/Q_{sim})}, \quad (4)$$

where C_{meas} is the measured atmospheric concentration, C_{bg} is the background concentration and C_{sim} is the predicted concentration for a simulation using the emission rate Q_{sim}.

One model based on this principle is the backwards Lagrangian stochastic (Ls) model of Flesch et al. (2004), which is implemented in the WindTrax software (Thunder Beach Scientific, Nanaimo, Canada). This model has been successfully applied to estimate emission rates using mean concentrations for averaging periods of less than 1 h (see e.g. Flesch et al., 2005) up to 26 h (Sommer et al., 2005).

The model of Flesch et al. (2004) also has the capability to be run forwards, i.e. the calculation of atmospheric concentrations from a known or estimated source emission rate. In this respect, the model functions similarly to other atmospheric dispersion models such as ADMS (Carruthers et al., 1994), AERMOD (Cimorelli et al., 2002) and LADD (Dragosits et al., 2002). All three of these models have been used to estimate emission rates of NH_3 sources by using an arbitrary emission rate in the model and then fitting the modelled atmospheric concentrations to the measured values (above background) by applying a correction factor (see e.g. Hill et al., 2008; Faulkner et al., 2007; Theobald et al., 2006). From Equation (4), the real emission rate (Q) is estimated to be the emission rate used in the simulation multiplied by the correction factor.

Three atmospheric dispersion models (ADMS 4.1, LADD and the Ls model of Flesch et al. (2004), implemented in WindTrax V.2.0.8.3) were used to estimate the ammonia emissions of the penguin colony. All three models simulate atmospheric dispersion processes in fundamentally different ways, as described in Appendix 1.

All three models were used to simulate the mean atmospheric concentration at the measurement locations closest to the colony (1–7; Fig. 1c) for the three measurement periods using an arbitrary constant emission rate of 1 μg NH_3 m^{-2} s^{-1}. Appendix 1 provides details of the model parameterisations used and the uncertainty analyses. The Ls model was also used in 'backwards' mode using the measured mean concentrations and hourly meteorological data as input to derive hourly emission estimates. Both the forwards and backwards simulations used the trajectories of fifty thousand "fluid particles" for each measurement location for each hour.

The forwards simulations (ADMS, LADD and the Ls model) assume that the colony emission rate is constant in time and the atmospheric concentrations vary temporally as a result of changing meteorological conditions. The backwards simulations of the Ls model, however, assume that the atmospheric concentrations are constant in time and that the emission rate varies temporally. Both of these assumptions are not realistic since the emission rate and the atmospheric concentrations will both vary temporally as result of changing meteorological conditions and penguin behaviour. However, this does not mean that the methodology cannot give a useful emission estimate. For example, Theobald et al. (2012) showed that the ADMS and LADD models predicted mean NH_3 concentrations near a pig farm to an acceptable degree of accuracy, even though a constant emission rate was used in the simulations. Due to the lack of emission estimates for penguin colonies in the literature, we believe that the application of these techniques has the potential to provide useful emission estimates, although the uncertainty introduced due to the assumptions made must be taken into account.

The emission rate estimated for each measurement period from the backwards Ls simulations was calculated as the mean value of the hourly emission estimates output by the model. For the forwards simulations of all three models, the concentration

Table 1
The performance measures used to optimise the predicted concentrations and their relationship to the observed (C_o) and predicted concentrations (C_p).

Performance measure	Definition	Optimum value
Fractional bias (FB)	$FB = \frac{2(\overline{C_o} - \overline{C_p})}{(\overline{C_o}+\overline{C_p})}$	0
Geometric Mean Bias (MG)	$MG = \exp(\overline{\ln C_o} - \overline{\ln C_p})$	1
Normalised mean square error (NMSE)	$NMSE = \frac{\overline{(C_o - C_p)^2}}{\overline{C_o}\,\overline{C_p}}$	0
Geometric variance (VG)	$VG = \exp[\overline{(\ln C_o - \ln C_p)^2}]$	1

predictions using the arbitrary emission rate (1 μg NH_3 m^{-2} s^{-1}) were compared with the measured values and then multiplied by a factor to fit the predicted concentrations to the measured values for each measurement period. This correction factor represented the ratio of the actual emissions to the emission rate used in the simulations and was determined by optimisation of four of the performance measures of Chang and Hanna (2004) (Table 1). These were optimised individually by adjusting the correction factor to either remove the bias (i.e. $MG = 1$ or $FB = 0$) or minimise the scatter (i.e. minimising *NMSE* or *VG*). By definition, *VG* is minimised when $MG = 1$ and so the same correction factor is obtained by the optimisation of both of these performance measures.

3. Results

3.1. Meteorological data

Due to the influence of the Cape Hallett peninsula, the predominant wind direction during all three measurement periods was from the southwest (Fig. 2). Table 2 shows the minimum, maximum and mean values for the wind speed, air temperature and solar radiation for the three measurement periods. Wind speeds were, on average, strongest during the first measurement period (for the period with available data) and weakest during the second, while mean air temperatures decreased throughout the experimental period.

Ten-degree wind-sector roughness lengths were calculated to be between 0.008 and 0.46 m (see Appendix 1). However, some of these values were calculated from very few records and were, therefore, not very reliable. A more robust z_0 estimate was calculated from the wind sectors that made up 95% of the data record (nine wind sectors), with a range of 0.008–0.034 m and a mean value of 0.020 m.

3.2. Measured and modelled atmospheric concentrations

For all measurement periods, a general decrease in measured concentrations with distance from the colony centre was observed (Fig. 3). Measured concentrations during the first period at the remote sites (8–11) were in the range 0.06–0.26 μg NH_3 m^{-3}.

Concentrations predicted by ADMS, LADD and the Ls model (forwards), using the arbitrary emission rate, were well correlated with the measured values ($R^2 = 0.69$–0.88, $R^2 = 0.62$–0.87 and $R^2 = 0.79$–0.91 for ADMS, LADD and the Ls model, respectively) (Fig. 4).

3.3. Emission calculations

3.3.1. Inverse dispersion modelling

For the forwards simulations, optimising the predictions of the three models using each performance measure individually gave the emission correction factors shown in Table 3. Since it is not possible to optimise more than one performance measure at a time (other than *MG* and *VG*) and since the correction factors are similar for all performance measures for each measurement period and model, the range of correction factor values was taken as the correction factor uncertainty.

All three models estimated a decrease in the correction factor (i.e. colony emission) going from Period 1 to Period 3. To take into account the uncertainty due to model input data (roughness length and deposition parameters, see Appendix 1), correction factors were also calculated for the predictions at both the lower and upper end of the concentration uncertainty ranges shown in Fig. 4. The three-model mean emission estimates (and 95% confidence intervals) were 4.4 (3.7–6.4), 1.9 (1.4–3.5) and 1.4 (1.1–2.4) μg m^{-2} s^{-1}, for the three periods respectively.

The backwards Ls model gave significantly larger ($P < 0.05$) mean emission rates (7.4, 8.2 and 3.6 μg m^{-2} s^{-1}, for the three periods respectively) than the optimisation of the forwards simulations, with 95% confidence intervals of 5.9–10.0, 5.4–11.5 and 2.6–4.7 μg m^{-2} s^{-1}, respectively.

3.3.2. Aerodynamic gradient method

The measured vertical concentration profiles are shown in Fig. 5. For the calculation of the fluxes using the aerodynamic gradient method, the concentration measured at the lowest height during Period 1 was not used because only one of the triplicate samples survived and that sample was damaged. The uncertainty in the

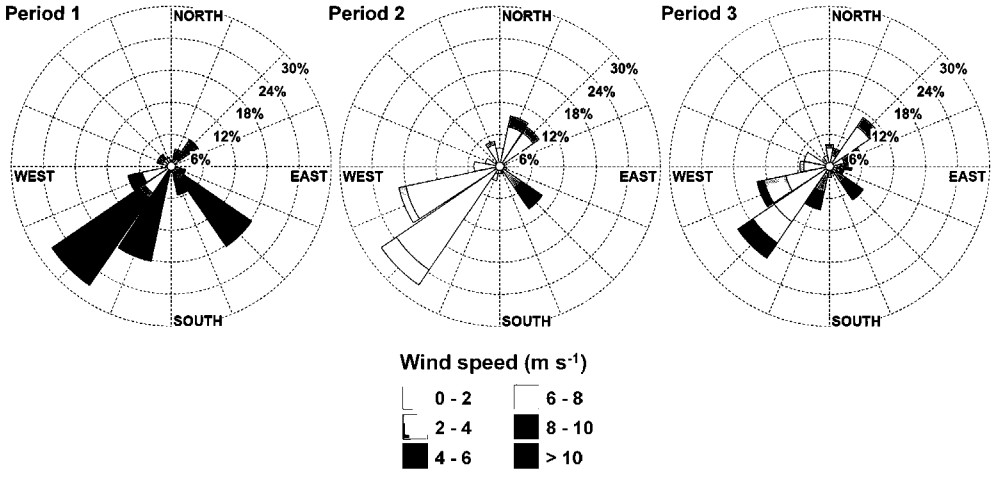

Fig. 2. Wind speed and wind direction frequency plots for the three measurement periods. Plotted using WRPLOT v7.0 (Lakes Environmental Software).

Table 2
Mean, minimum and maximum values of selected meteorological variables for each measurement period.

Measurement period	Wind speed ($m\ s^{-1}$)		Air temperature (°C)		Solar radiation ($W\ m^{-2}$)	
	Mean	Min Max	Mean	Min Max	Mean	Min Max
1) 26/12/2005– 10/01/2006	6.8	0.2 16.6	−0.5	−6.0 2.8	232	10 830
2) 11–17/01/2006	1.6	0.3 6.4	−1.0	−5.8 2.1	298	12 761
3) 17–23/01/2006	2.3	0.2 6.9	−1.9	−7.5 0.6	225	5 761

emission estimates was estimated from the 95% confidence intervals of the roughness length and the slopes of the linear regressions shown in Fig. 5. The mean emission estimates (and 95% confidence intervals) were 5.5 (4.6–7.0), 1.3 (0.6–2.3), 1.1 (0.5–2.0) $\mu g\ m^{-2}\ s^{-1}$, for the three periods respectively.

3.3.3. Emission estimate summary

The emission per penguin breeding pair was calculated from the source emission estimates using the colony population data and surface area of the colony, for each of the estimation methods (three dispersion models and the aerodynamic gradient). These calculations resulted in a range of emission estimates from 0.8 to 6.0 g NH_3 per breeding pair per day with varying degrees of uncertainty (Fig. 6), with the largest emission estimates from the backwards simulations of the Ls model. Breeding pair numbers were used to scale the colony emission rate since they are the only population data available. However, it must be borne in mind that the emission rate per breeding pair will also include contributions from non-breeding adults and chicks.

All three forwards models and the aerodynamic gradient calculations estimate a larger emission rate for the first measurement period than for the second and third periods. This is primarily due to the larger mean wind speed for this measurement period. However, only about half of the measurement period was simulated due to anemometer failure and, therefore, it is not known whether these larger mean wind speeds were typical for the entire measurement period or only for the second half. Due to this uncertainty, the simulations of the first measurement period provide less reliable emission estimates, while remaining useful for comparison.

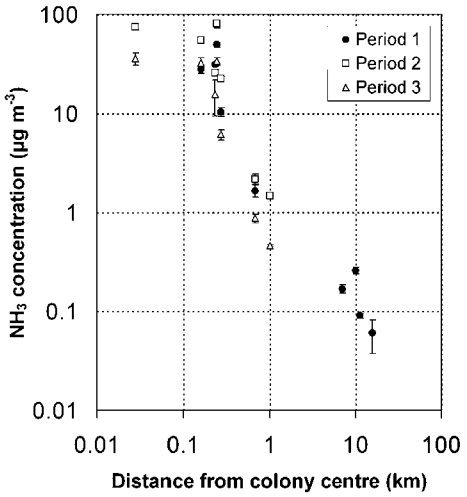

Fig. 3. Measured mean ammonia concentrations versus distance from the colony centre for all three measurement periods plotted on log–log axes. Error bars indicate ± two standard deviations of the triplicate ALPHA sampler values. The colony centre is defined as the geometric centre of the wide part of Seabee Hook (approximately 30 m south-west of site 1).

4. Discussion

4.1. Method applicability and best estimate of emission rate

The reasonable agreement between the emission estimates obtained from the three forwards dispersion models (ADMS, LADD and the Ls model) is encouraging. The three models simulate the main dispersion processes in different ways and the fact that the resulting emission estimates are similar and are of the same order of magnitude as those from the aerodynamic gradient approach gives some confidence in these estimates. It can be assumed, therefore, that all three models are suitable for this type of inverse modelling case study (i.e. ground level area source, flat terrain and long concentration averaging periods). This assumption is also in agreement with Theobald et al. (2012) who demonstrated good agreement between the concentration predictions of ADMS and LADD for agricultural ground-level area sources.

The emission estimates derived from the forwards and backwards Ls model are significantly different ($P < 0.05$) due to the different assumptions made (constant emission rate vs. constant atmospheric concentrations), which affect the way the mean emission rate is calculated.

To test the validity of the first assumption (constant emission rate and varying atmospheric concentrations), the forwards simulations were re-run assuming that the emission rate during the simulation was dependent on air temperature (T) and wind speed (u):

$$Q_{var} = Ae^{(0.07T)}e^{(0.042u)}; \quad (5)$$

where A is a constant and the coefficients for air temperature (0.07) and wind speed (0.042) were taken from Zhu et al. (2011) and Søgaard et al. (2002), respectively. The variable emission rate was then normalised so that the average emission for each measurement period was unity (Fig. 7). The normalised emission rate varied from 0.6 to 1.5 throughout the three measurement periods with a ratio of mean day-time maximum to mean night-time minimum emission rates of 1.5. Additional simulations were also carried out with different ratios of day-time to night-time emission rates up to a ratio of 8 (similar to the modelled and measured emission time series for Macaroni Penguins on Bird Island in the South Atlantic from Riddick et al. (2012)), in order to evaluate the effect of the simulated diurnal variability on the emission estimates (Fig. 7).

For the two measurement periods with complete meteorological data (Periods 2 and 3), the mean emission estimates calculated from these simulations were up to 73% larger than the estimates from the constant emission simulations (Fig. 8), although they were still significantly smaller than those calculated from the backwards simulations. This suggests that the use of a constant emission rate in the

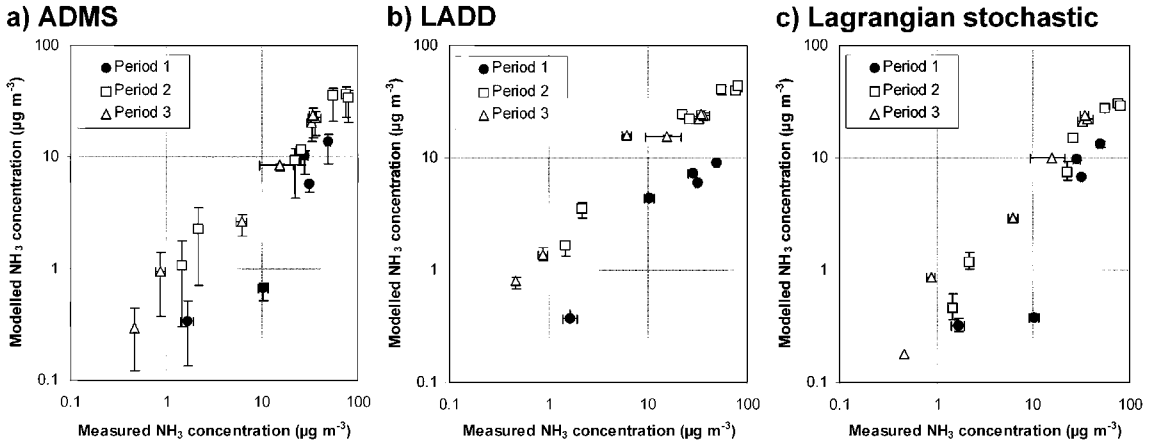

Fig. 4. Modelled versus measured NH_3 concentrations on log–log axes for the 'forwards' simulations of a) ADMS; b) LADD and c) Ls model for all three measurement periods, with the models run using an arbitrary emission rate of 1 µg NH_3 m^{-2} s^{-1}. Error bars indicate ± two standard deviations of the triplicate measured values and the 5th and 95th percentile concentrations from the uncertainty analysis of the modelled values (see Appendix 1).

Table 3
Emission correction factors obtained by optimising the performance measures *MG*, *VG*, *FB* and *NMSE* for all three forwards models and for all three measurement periods. These correction factors are derived from simulations using an arbitrary emission rate of 1 µg NH_3 m^{-2} s^{-1}.

Model	Performance measure	Correction factor for measurement period:		
		1	2	3
ADMS	*MG* and *VG*	5.2	1.8	1.6
	FB	3.9	2.0	1.6
	NMSE	3.6	2.0	1.5
LADD	*MG* and *VG*	4.1	1.2	0.9
	FB	4.4	1.5	1.2
	NMSE	4.7	1.6	1.3
Ls	*MG* and *VG*	5.8	2.3	1.6
	FB	3.9	2.4	1.5
	NMSE	3.7	2.4	1.5

simulations may underestimate emissions by up to 40%. Although this introduces substantial uncertainty into the emission estimates, this uncertainty is a similar order of magnitude to the uncertainty of the emission estimates of the other methods (Figs. 6 and 8).

The fact that the inclusion of a more realistic emission rate gives comparable emission estimates to those from the constant emission simulations suggests that the constant emission rate assumption is more valid than the assumption of constant atmospheric concentrations. This conclusion is also backed-up by the fact that the forwards Ls simulations gave similar emission estimates to the other two models and the aerodynamic gradient method.

The aerodynamic gradient method applied here assumes that neutral conditions dominated during the measurement periods in order to ignore the stability corrections of Equations (1) and (2). In order to explore this assumption further, we assessed the range of hourly values of the friction velocity (u_*) calculated from the hourly meteorological data using the method of Holtslag and Van Ulden (1983), taking into account stability corrections. For example, during measurement period 2, the calculated u_* ranged from 0.0046 to 0.54 m s^{-1}, with a 5th–95th percentile range of 0.012–0.30 m s^{-1} and a median value of 0.137 m s^{-1}. The value of u_* calculated for neutral conditions and used in Equation (3) to represent the entire measurement period (0.131 m s^{-1}) differs by only 5% from the median value of the hourly calculated values, indicating that values lower and higher than the neutral value occurred with a similar frequency during the measurement period.

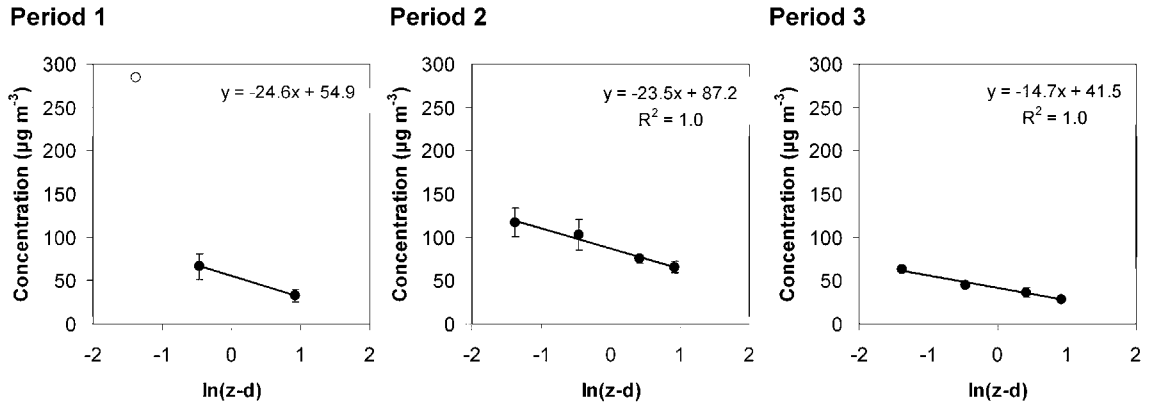

Fig. 5. Measured vertical concentration profiles plotted on a logarithmic height axis for the three sampling periods. The concentration measured at the lowest height during Period 1 (open symbol) was excluded from the analysis. Error bars indicate ± two standard deviations of the triplicate measured values. N.B. the displacement height (d) is assumed to be zero.

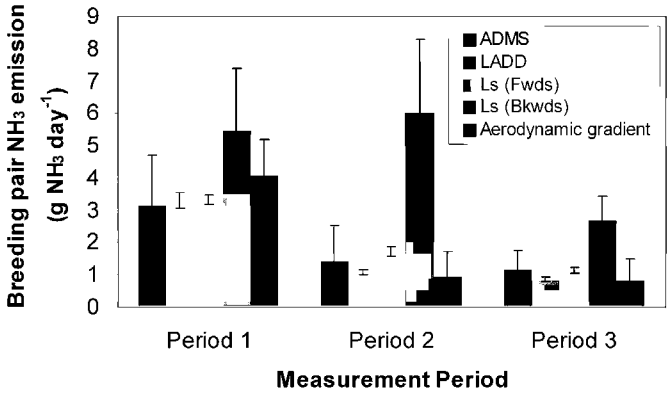

Fig. 6. Penguin breeding pair ammonia emission estimates calculated from the simulations of the three models and the aerodynamic gradient method for all three measurement periods. The error bars indicate the uncertainty in the ADMS, LADD and Ls model estimates due to uncertainty in the surface parameters and the uncertainty in the vertical profile calculations due to uncertainty in z_0 and the slopes of the logarithmic concentration profiles.

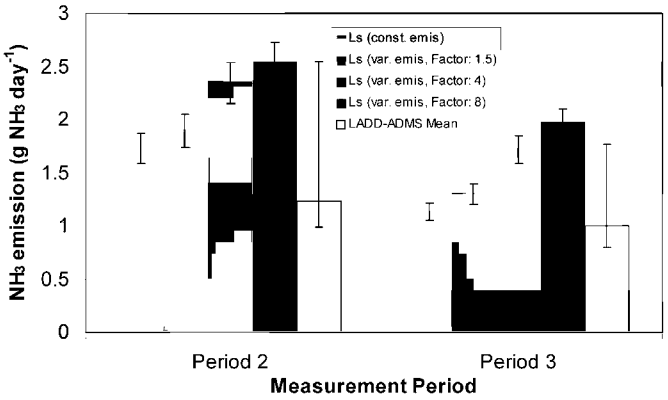

Fig. 8. Penguin breeding pair ammonia emission estimates for measurement periods 2 and 3 calculated with the forwards Ls model using constant emission rates and emission rates with ratios of mean day-time maxima to mean night-time minima of 1.5, 4 and 8. The mean emission estimate of the other two models (LADD and ADMS) and the range of emission estimates from both of these models are also shown for comparison.

With regards to the concentration vertical gradient, it would be expected that during the measurement period concentration gradients smaller and larger than the measured mean gradient occurred. If the emission estimate were to be calculated on an hourly basis using Equation (3) ($F = -u_* C_*$), it would not be unreasonable to expect that the net effect would be an emission estimate similar to that calculated by assuming neutral conditions and the mean concentration gradient, due to cancelling-out of periods with high and low values of u_*. However, this may not be the case due to correlation between u_* and C_*. Without hourly concentration gradient measurements it is not possible to evaluate this assumption thoroughly and we recommend an evaluation of the effect of different averaging periods on the aerodynamic gradient emission estimates as a focus for further work. However, the fact that this method gave similar emission estimates to the forwards dispersion simulations, suggests that it is a valid assumption.

The best (most robust) estimate of penguin emissions, therefore, can be obtained by considering the constant emission simulations of the three forwards dispersion models and the aerodynamic gradient method. For the measurement periods with reliable meteorological data throughout (second and third), the mean emission is 1.1 g NH_3 per breeding pair per day with a 95% confidence interval of 0.4–2.5 g NH_3 per breeding pair per day. If the forwards Ls simulations with varying emissions and a ratio of 8 between the mean daily maxima and minima are used, the resulting best emission estimate is only slightly different (1.3 g NH_3 per breeding pair per day with a 95% confidence interval of 0.4–2.7 g NH_3 per breeding pair per day).

4.2. Comparison with bioenergetics model

The emission estimates obtained agree well with that calculated using the temperature-dependent bioenergetics model of Riddick et al. (2012), which gives an emission estimate for Cape Hallett of 2.0 g NH_3 per breeding pair per day for the mean air temperature measured during Periods 2 and 3 (−1.5 °C). This is encouraging since the inverse modelling approach and the bioenergetics method are completely independent estimates using top-down and bottom-up approaches, respectively. Based on an in-colony excretion rate of 50 g N per day per breeding pair for Adélie penguins

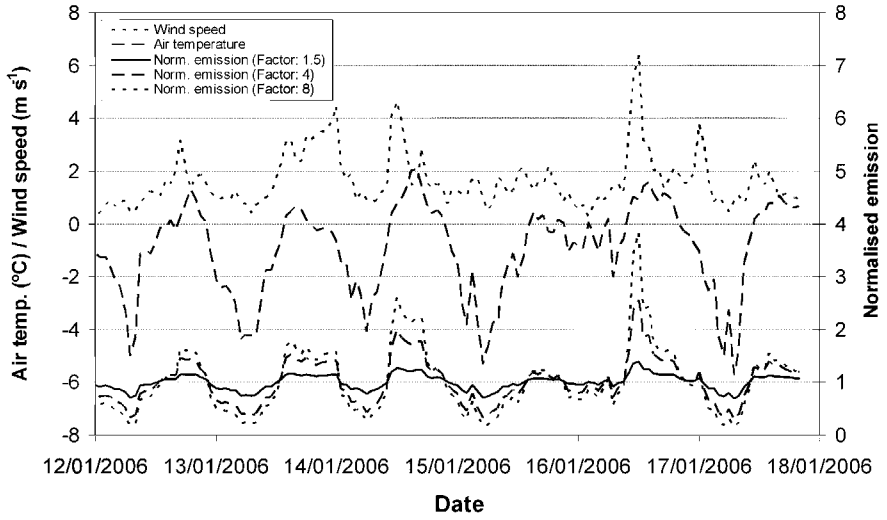

Fig. 7. Measured air temperature and wind speed and calculated normalised emission rate for sampling period 2. Three normalised emission rates are shown corresponding to ratios of mean day-time maxima to mean night-time minima of 1.5, 4 and 8.

(Riddick, pers. comm.), the present results equate to a loss of 1.9% (95% confidence interval: 0.6–4.2%) of the excreted guano N. This fractional loss is much smaller than the 36% volatilisation rate estimated by Blackall et al. (2007) for a Gannet colony (Bass Rock) in temperate UK conditions, and points to a high temperature dependence of NH_3 emission rates (Sutton et al., 2013). Zhu et al. (2011) estimated a total loss of 0.12% of N from Adélie penguin guano during five eight-hour thawing periods in the laboratory. However, even after the five thawing periods the guano emissions were only reduced by about 50%, suggesting that long term losses could be substantially larger. Zhu et al. (2011) did not simulate the effects of varying wind speed or the influence of solar radiation, both of which could also affect the emission rate. In addition, total nitrogen content of the guano used in the laboratory experiments (1.08–3.60%) was lower than that found by Hofstee et al. (2006) in the surface layer of the Adélie penguin mounds of Seabee Hook (8.9–14.5%), which could also explain why the estimated NH_3 losses from Seabee Hook were larger than those observed by Zhu et al. (2011).

4.3. Uncertainties in the emission estimates

The calculated uncertainty in the inverse modelling and aerodynamic gradient estimates is due to differences between the predictions by the different models as well as the uncertainty in surface parameters (roughness length and dry deposition parameters) and vertical concentration profiles.

There are other sources of uncertainty, however, the influences of which are more difficult to estimate. For example, the number of breeding pairs in the colony varies annually and the 2005/2006 emission estimates were made assuming a colony size equal to the last available breeding pair count (39 000 breeding pairs in 1998/1999). Counts during the last 50 years have varied between 37 600 and 66 300 breeding pairs, peaking in 1987 (Landcare Research, 2000). During the period between the two most recent counts (1991 and 1998), the colony population decreased by an average of about 700 breeding pairs per year. If we assume that the colony continued to decrease at this rate between 1998 and 2005, then the colony population would have decreased by about 13% during this period. The assumption of a stable colony population, therefore, would result in an underestimate of the emission per breeding pair of about 13%. Uncertainty in penguin numbers at the site is, therefore, probably a small source of error compared with other factors.

Another assumption made in the above emission estimates with the forwards models is that of a constant emission rate. In reality the emission rate will depend on many environmental and biological factors, such as ground/air temperature, wind speed, solar radiation, penguin movements and feeding/excretion habits. With regards to the environmental factors, the assumption of a constant emission probably underestimates day-time emissions and overestimates night-time emissions due to the higher temperatures, wind speeds and solar radiation during the day. Since modelled mean atmospheric concentrations are often strongly influenced by calm night-time periods (Theobald et al., 2012), an overestimation of night-time emissions will most likely lead to an overestimation of atmospheric concentrations and hence an underestimation of the emission rate. This hypothesis was tested by including time-varying emissions in the Ls simulations, which suggested that the use of a constant emission rate may underestimate emissions by up to 40%. However, although the simple emission model used provides more realistic emission estimates than a constant value, exactly how realistic this model is remains unclear. The temperature dependence of the emission model is taken from the laboratory measurements by Zhu et al. (2011) but the temperature range used (4–30 °C) did not cover that observed at Cape Hallett during the measurement periods (−8 to 3 °C) and so may not adequately represent the effects of freezing–thawing cycles on the emission rate. The effects of precipitation and/or the moisture content of the penguin guano and colony soil surface layer are also not taken into account in the emission model. The wind speed dependence of the simple emission model was taken from the ALFAM agricultural slurry spreading model (Søgaard et al., 2002). Although similar processes are responsible, it cannot be assumed that penguin emissions have a similar wind speed dependence.

The assumption of a spatially homogeneous emission rate is another potential source of model uncertainty, since field observations show that the penguin nests are actually arranged in several groupings throughout the colony. However the use of multiple measurement locations including some distant from the source should have helped to minimise this uncertainty.

5. Conclusions

The application of inverse-dispersion modelling and the aerodynamic gradient method gave a best estimate of ammonia emissions from an Adélie penguin colony in Antarctica of 1.1 g NH_3 per breeding pair per day with a 95% confidence interval of 0.4–2.5 g NH_3 per breeding pair per day for periods with a mean air temperature of −2 to −1 °C;.

This estimate is in good agreement with that from a bioenergetics model (2.0 g NH_3 per breeding pair per day). Based on a daily estimated excretion rate of 50 g N per breeding pair, the estimates here equate to a volatilisation of 1.9% (95% confidence interval: 0.6–4.2%) of the excreted nitrogen. This rate of volatilisation is much smaller than seen in temperate bird colonies pointing to a substantial temperature dependence of NH_3 emission.

Emission estimates calculated from forwards and backwards simulations of the Lagrangian stochastic (Ls) model differed significantly due to the different assumptions made (constant emission rate and constant atmospheric concentration, respectively). Optimisation of the forward simulations with measurements gave the closest agreement to the estimates made using other dispersion models and the aerodynamic gradient method.

The forwards and backwards Ls estimates depend on the assumptions of a constant emission rate or constant atmospheric concentrations, respectively. The use of an empirical emission model in the forwards simulations gave higher emission estimates than the constant emission simulations, although the estimates were not significantly different to those obtained from the other forwards models. This suggests that the assumption of a constant emission rate is more valid than an assumption of constant atmospheric concentrations, in this case study.

Although the emission rates estimated using these methods contain considerable uncertainty due to the assumptions made and the uncertainty of the model input data, the results clearly demonstrate how the fraction of excreted N volatilised as NH_3 is an order of magnitude less in this Antarctic context than previously measured for temperate seabird colonies.

Acknowledgements

This research was supported by grants gratefully received from The Royal Society (to PDC) and the Natural Environment Research Council (to PDC and MAS). MRT and MAS are grateful for the financial support from the European Commission Projects: NitroEurope and ÉCLAIRE. PDC thanks Allan Green (School of Biology, University of Waikato) for the invitation to participate in ANZ's (Antarctic New Zealand's) Latitudinal Gradient Project and ANZ for provision of travel, accommodation and research facilities at Scott

Base and Cape Hallett. We thank Rachel Brown and Gus McAllister for facilitating research activities at Cape Hallett. MRT also thanks Stuart Riddick for providing the parameterisation of the bio-energetics model.

Appendix 1. Models used, parameterisations and uncertainty analyses

The three atmospheric dispersion models used in this study simulate atmospheric dispersion in fundamentally different ways.

ADMS (Atmospheric Dispersion Modelling System) is an 'advanced' Gaussian dispersion model that calculates atmospheric dispersion based on modified versions of the Gaussian plume equation, taking into account vertical profiles of boundary layer parameters and continuous stability functions (Carruthers et al., 1994). The model uses hourly meteorological and emission data to predict hourly and/or long-term mean atmospheric concentrations and deposition rates.

LADD (Local Area Dispersion and Deposition) is a statistical Lagrangian model that simulates atmospheric dispersion and dry deposition by moving a vertical column of air along straight-line trajectories across a grid (Dragosits et al., 2002). Model input is in the form of mean wind speed and wind direction probabilities for each 10° wind sector, and the mean emission rate of each grid square. The model outputs mean atmospheric concentrations at several heights and mean dry deposition rates to each grid square.

The Lagrangian stochastic (Ls) model of Flesch et al. (2004) simulates atmospheric dispersion by following infinitesimal air parcels or 'fluid particles' as they move through the atmosphere. A particle trajectory through the atmosphere can be thought to be composed of small changes in particle position and velocity as a result of atmospheric turbulence. These changes are predicted through the equations of Lagrangian stochastic motion, which are used to simulate the transport of gases from an emission source to a receptor location (or vice versa). The model uses hourly (or more frequent) meteorological data plus emission data (in forwards mode) or atmospheric concentration data (in backwards mode), in order to predict atmospheric concentrations or emission rates, respectively.

Model surface parameters

All three dispersion models require an estimate of the aerodynamic roughness length (z_0) for the domain. For the rocky land cover where the colony and meteorological station were located, z_0 was estimated from the wind gust data for the whole of 2005 using the method recommended by the US EPA (US EPA, 1987), which uses the empirical relationship of Wieringa (1993). The value of z_0 estimated in this way was used for the entire domain for the Ls model since only one value of z_0 can be used by the model for each simulation. ADMS and LADD, on the other hand, can use spatially varying values of z_0, corresponding to the different land cover types within the modelling domain. However, this option in ADMS (v4.1) requires the use of the complex terrain model option, which imposes limits on the turbulence and does not allow the atmosphere to become very stable. Testing this option in ADMS gave emission estimates an order of magnitude larger than the other methods (LADD, Ls model and the atmospheric gradient method) and so it was concluded that the constant z_0 for the entire domain was a more realistic approach. This decision was justified because the core dispersion domain (i.e. the colony and the measurement locations around its perimeter) was relatively flat; hence a limitation of atmospheric stability in this key part of the domain would not be appropriate. Spatially varying values of z_0 were used in LADD, which assumes a flat domain. Land cover classification data were obtained from the Antarctic Digital Database by the Scientific Committee on Antarctic Research (ADD Consortium, 2000). The values of z_0 used for the different land cover types are listed in Table A1.

The simulations of ADMS and LADD also estimated the loss of ammonia due to dry deposition, whereas the Ls model does not simulate this process. The LADD simulations used land cover-specific values of canopy resistance (R_c) (Table A1), whereas ADMS (v4.1) requires a fixed dry deposition velocity for the entire domain. This dry deposition velocity was estimated to be 1×10^{-3} m s^{-1}. The justification for the use of this value was that the dry deposition rate to a non-vegetated rocky penguin colony would be substantially lower than that to semi-natural vegetation (with dry deposition velocities of a few mm s^{-1} under high concentration conditions (e.g. Cape et al., 2008)).

However, the values of both z_0 and dry deposition parameters used in these two models are highly uncertain due to the unusual nature of the modelling domain and so an uncertainty analysis was carried out assuming 95% confidence intervals for z_0 and the dry deposition parameters (canopy resistance in LADD and dry deposition velocity in ADMS) of ± a factor of three and ± a factor of ten, respectively. The factor of three for the z_0 values was taken from Hanna et al. (2007), who used a similar estimate of the uncertainty of z_0 values for the simulation of the dispersion of air pollutants in the Houston ship channel area. The factor of ten for the deposition parameters was chosen based on expert judgement due to the lack of information on deposition processes for this type of environment.

The values of R_c listed in Table A1 assume that snow- and ice-covered surfaces are wet. However, at temperatures below zero this may not be the case and the R_c values could be substantially larger, which justifies an uncertainty analysis over a large range of values.

Log-normal distributions were assumed for the values of z_0 and the deposition parameters and a Monte Carlo analysis was carried out by randomly sampling the two distributions for 100 scenarios for each model and for each measurement period.

Table A1
Surface parameters used in the LADD simulations

Land cover category	Roughness length (z_0) [m]	Canopy resistance (R_c) [s m^{-1}]
Snow-covered rock	0.02[a]	1[b]
Bare rock (coast)	0.02[a]	1000[b]
Bare rock (mountains)	2.0[c]	1000[b]
Ice	0.01[d]	1[b]
Sea	0.001[e]	0.1[b]

[a] Calculated in this study.
[b] Expert judgement.
[c] Moderate mountainous areas (Stull, 1988).
[d] Sea ice z_0 range: 0.005–0.04 m (Mote and O'Neill, 2000).
[e] Open water z_0 range: 0.0001–0.01 m (Richards, 1997).

Meteorological data

For the LADD model, the 15-min wind speed and wind direction data were converted to wind roses consisting of the wind direction frequency and mean wind speed for each ten degree wind sector for each sampling period. Hourly mean values of air temperature, relative humidity, solar radiation, wind speed, wind direction and the standard deviation of the wind direction were used as input to ADMS. The Ls model used hourly mean wind speed and wind direction data.

To represent the thermal stratification of the atmosphere in ADMS and the Ls model, the Monin–Obukhov length (L) was calculated from the hourly values of wind speed and solar radiation using the method of Holtslag and Van Ulden (1983). This method is not valid for periods of very stable conditions, for which a value of $L = 10$ m was assumed.

References

ADD Consortium, 2000. Antarctic Digital Database, Version 3.0. Database, Manual and Bibliography. Scientific Commission on Antarctic Research, Cambridge, U.K.

Blackall, T.D., Wilson, L.J., Theobald, M.R., Milford, C., Nemitz, E., Bull, J., Bacon, P.J., Hamer, K.C., Wanless, S., Sutton, M.A., 2007. Ammonia emissions from seabird colonies. Geophys. Res. Lett. 34, 10801.

Cape, J., Jones, M., Leith, I., Sheppard, L., Van Dijk, N., Sutton, M., Fowler, D., 2008. Estimate of annual NH_3 dry deposition to a fumigated ombrotrophic bog using concentration-dependent deposition velocities. Atmos. Environ. 42, 6637–6646.

Carruthers, D., Holroyd, R., Hunt, J., Weng, W., Robins, A., Apsley, D., Thompson, D., Smith, F., 1994. UK-ADMS: a new approach to modelling dispersion in the earth's atmospheric boundary layer. J. Wind Eng. Ind. Aerodyn. 52, 139–153.

Chang, J.C., Hanna, S.R., 2004. Air quality model performance evaluation. Meteorol. Atmos. Phys. 87, 167–196.

Cimorelli, A.J., Perry, S.G., Venkatram, A., Weil, J.C., Paine, R.J., Wilson, R.B., Lee, R.F., Peters, W.D., Brode, R.W., Pauimer, J.O., 2002. AERMOD: Description of Model Formulation Version 02222.

Dragosits, U., Theobald, M.R., Place, C.J., Lord, E., Webb, J., Hill, J., ApSimon, H.M., Sutton, M.A., 2002. Ammonia emission, deposition and impact assessment at the field scale: a case study of sub-grid spatial variability. Environ. Pollut. 117, 147–158.

Famulari, D., Fowler, D., Hargreaves, K., Milford, C., Nemitz, E., Sutton, M., Weston, K., 2004. Measuring eddy covariance fluxes of ammonia using tunable diode laser absorption spectroscopy. Water Air Soil Pollut. Focus 4, 151–158.

Famulari, D., Fowler, D., Nemitz, E., Hargreaves, K.J., Storeton-West, R., Rutherford, G., Tang, Y.S., Sutton, M.A., Weston, K.J., 2010. Development of a low-cost system for measuring conditional time-averaged gradients of SO_2 and NH_3. Environ. Monit. Assess. 161, 11–27.

Faulkner, W.B., Powell, J.J., Lange, J.M., Shaw, B.W., Lacey, R.E., Parnell, C.B., 2007. Comparison of dispersion models for ammonia emissions from a ground-level area source. Trans. ASAE 50, 2189–2197.

Flesch, T., Wilson, J., Harper, L., Crenna, B., Sharpe, R., 2004. Deducing ground-to-air emissions from observed trace gas concentrations: a field trial. J. Appl. Meteorol. 43, 487–502.

Flesch, T.K., Wilson, J.D., Harper, L.A., Crenna, B.P., 2005. Estimating gas emissions from a farm with an inverse-dispersion technique. Atmos. Environ. 39, 4863–4874.

Hanna, S.R., Paine, R., Heinold, D., Kintigh, E., Baker, D., 2007. Uncertainties in air toxics calculated by the dispersion models AERMOD and ISCST3 in the Houston ship channel area. J. Appl. Meteorol. Climatol. 46, 1372–1382.

Hill, R., Smith, K., Russell, K., Misselbrook, T., Brookman, S., 2008. Emissions of ammonia from weeping wall stores and earth-banked lagoons determined using passive sampling and atmospheric dispersion modelling. J. Atmos. Chem. 59, 83–98.

Hofstee, E.H., Balks, M.R., Petchey, F., Campbell, D.I., 2006. Soils of Seabee Hook, Cape Hallett, Northern Victoria Land, Antarctica. Antarct. Sci. 18, 473.

Holtslag, A.A.M., Van Ulden, P., 1983. A simple scheme for daytime estimates of the surface fluxes from routine weather data. J. Clim. Appl. Meteorol. 22, 517.

Landcare Research, 2000. Adélie Penguin Census Data. http://www.landcareresearch.co.nz/resources/data/adelie-census-data.

Lindeboom, H.J., 1984. The nitrogen pathway in a penguin rookery. Ecology 65, 269–277.

Mote, P., O'Neill, A., 2000. Numerical Modeling of the Global Atmosphere in the Climate System. Springer.

McGinn, S., Janzen, H., 1998. Ammonia sources in agriculture and their measurement. Can. J. Soil Sci. 78, 139–148.

Misselbrook, T., Nicholson, F., Chambers, B., Johnson, R., 2005. Measuring ammonia emissions from land applied manure: an intercomparison of commonly used samplers and techniques. Environ. Pollut. 135, 389–397.

Richards, P.J., 1997. The effect of wind profile and twist on downwind sail performance. J. Wind Eng. Ind. Aerodyn. 67–68 (0), 313–321.

Riddick, S.N., Dragosits, U., Blackall, T.D., Daunt, F., Wanless, S., Sutton, M.A., 2012. The global distribution of ammonia emissions from seabird colonies. Atmos. Environ. 55, 319–327.

Søgaard, H.T., Sommer, S.G., Hutchings, N., Huijsmans, J., Bussink, D., Nicholson, F., 2002. Ammonia volatilization from field-applied animal slurry—the ALFAM model. Atmos. Environ. 36, 3309–3319.

Sommer, S.G., McGinn, S., Flesch, T., 2005. Simple use of the backwards lagrangian stochastic dispersion technique for measuring ammonia emission from small field-plots. Eur. J. Agron. 23, 1–7.

Stull, R.B., 1988. An Introduction to Boundary Layer Meteorology. Kluwer Academic Publishers.

Sutton, M.A., Nemitz, E., Milford, C., Fowler, D., Moreno, J., San Jose, R., Wyers, G.P., Otjes, R.P., Harrison, R., Husted, S., Schjoerring, J.K., 2000. Micrometeorological measurements of net ammonia fluxes over oilseed rape during two vegetation periods. Agric. For. Meteorol. 105, 351–369.

Sutton, M.A., Reis, Stefan, Riddick, S.N., Dragosits, Ulrike, Nemitz, Eiko, Theobald, M.R., Tang, Y.S., Braban, C.F., Vieno, Massimo, Dore, A.J., Mitchell, R.F., Wanless, Sarah, Daunt, Francis, Fowler, David, Blackall, T.D., Milford, Celia, Flechard, C.R., Loubet, Benjamin, Massad, Raia, Cellier, Pierre, Coheur, P.F., Clarisse, Lieven, van Damme, Martin, Ngadi, Yasmine, Clerbaux, Cathy, Skjøth, C.A., Geels, Camilla, Hertel, Ole, Wichink Kruit, Roy, Pinder, R.W., Bash, J.X., Walker, J.D., Simpson, Dave, Horvath, Laszlo, Misselbrook, T.H., Bleeker, Albert, Dentener, Frank, de Vries, Wim, 2013. Toward a climate-dependent paradigm of ammonia emission & deposition. R. Soc. London. Philos. Trans. B Biol. Sci. 368.

Tang, Y., Cape, J., Sutton, M.A., 2001. Development and types of passive samplers for monitoring atmospheric NO_2 and NH_3 concentrations. Sci. World 1, 513–529.

Theobald, M.R., Crittenden, P.D., Hunt, A.P., Tang, Y.S., Dragosits, U., Sutton, M.A., 2006. Ammonia emissions from a cape fur seal colony, cape cross, Namibia. Geophys. Res. Lett. 33 (3), L03812.

Theobald, M.R., Løfstrøm, P., Walker, J., Andersen, H.V., Pedersen, P., Vallejo, A., Sutton, M.A., 2012. An intercomparison of models used to simulate the short-range atmospheric dispersion of agricultural ammonia emissions. Environ. Model. Softw. 37, 90–102.

US EPA, 1987. On-site Meteorological Program Guidance for Regulatory Modeling Applications. USEPA, Research Triangle Park, North Carolina. EPA-450/4-87-013.

Wieringa, J., 1993. Representative roughness parameters for homogeneous terrain. Bound.-layer Meteorol. 63, 323–363.

Wilson, L.J., Bacon, P.J., Bull, J., Dragosits, U., Blackall, T.D., Dunn, K.C., Hamer, K.C., Sutton, M.A., Wanless, S., 2004. Modelling the spatial distribution of ammonia emissions from seabirds in the UK. Environ. Pollut. 131, 173–185.

Zhu, R., Sun, J., Liu, Y., Gong, Z., Sun, L., 2011. Potential ammonia emissions from penguin guano, ornithogenic soils and seal colony soils in coastal Antarctica: effects of freezing–thawing cycles and selected environmental variables. Antarct. Sci. 23, 78–92.